

Electronic Supplementary Information (ESI)

Formation of Kinetically Trapped Small Clusters of PEGylated Gold Nanoparticles Revealed by the Combination of Small-angle X-ray Scattering and Visible Light Spectroscopy

Daniel P. Szekrényes,¹ Cyrille Hamon,² Doru Constantin,^{2,3*} András Deák^{1*}

¹ Centre for Energy Research, Budapest, Hungary

² Université Paris-Saclay, CNRS, Laboratoire de Physique des Solides, 91405 Orsay, France

³ Institut Charles Sadron, CNRS and Université de Strasbourg, 67034 Strasbourg, France

Corresponding Author

*Doru Constantin: constantin@unistra.fr

*András Deák: andras.deak@ek-cer.hu

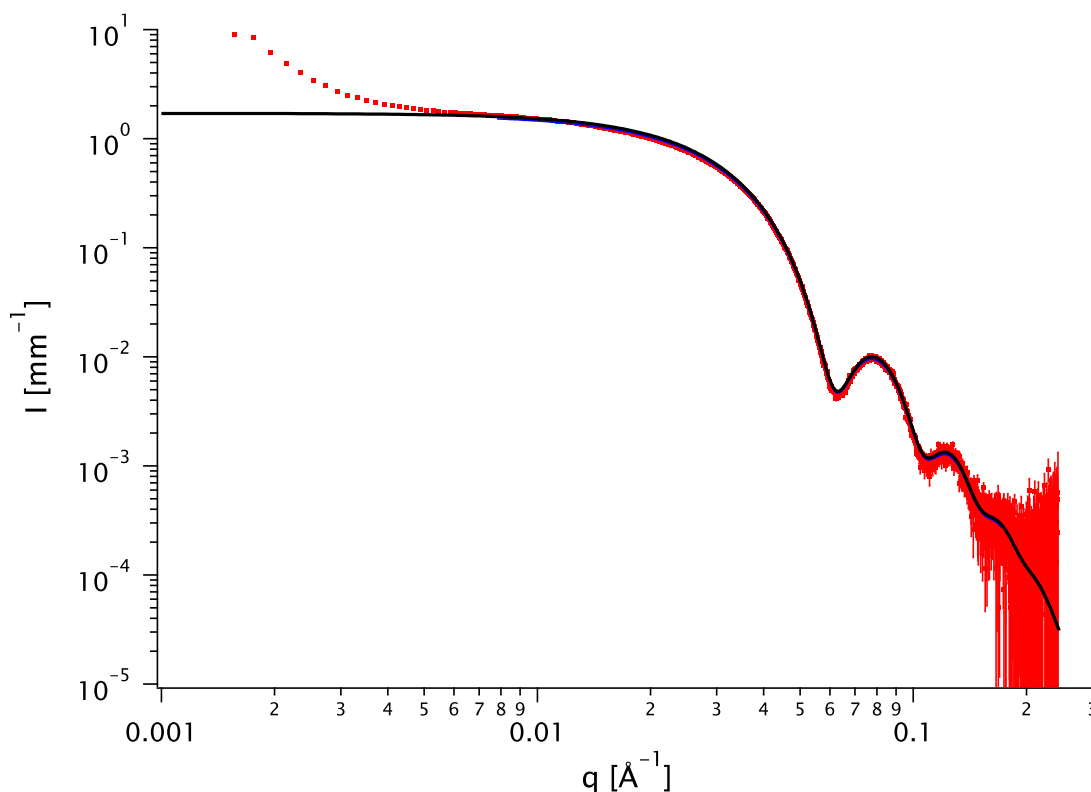


Figure S1: SAXS signal of PEGylated gold nanospheres well dispersed in water (symbols) and fit with a polydisperse sphere model (solid line).

The intensity scattered by the gold nanoparticles in dilute aqueous solution was fitted with a polydisperse sphere model (the polydispersity was described by a Schulz distribution). The mean diameter is $\langle 2a \rangle = 14.2$ nm and the standard deviation $\sigma = 1.3$ nm. The number concentration of the particles is $n_p = 6.5 \cdot 10^{-9} \text{ nm}^{-3}$, corresponding to a volume fraction $\varphi_p = 10^{-5}$. In the model we also use the appropriate scattering length density for gold and water at 16 keV: 108.2 and 9.44 \AA^{-2} , respectively.

Renormalization of the extinction spectra

For aggregating plasmonic nanoparticle systems, the time evolution of the extinction spectrum change might contain both the effect of plasmon coupling (in the form of red-shift and eventual appearance of new extinction modes) and sedimentation (extinction decrease). As the extinction measured at 400 nm is depending only on the concentration of Au⁰ in the light path, renormalizing the spectra at this wavelength can help to separate these two effects. Two examples are shown below. **Figure S2a** and **b** contain the raw extinction spectra. The extracted values at 400 nm are shown in **Figure S2c** and **d**. Due to the fluctuation, these time-dependent values are fitted with a linear curve; the parameters of which can be used to renormalize the extinction spectra at any arbitrary time. The result of the renormalization procedure is shown in **Figure S2e-f**, showing the impact of clustering on the extinction spectra.

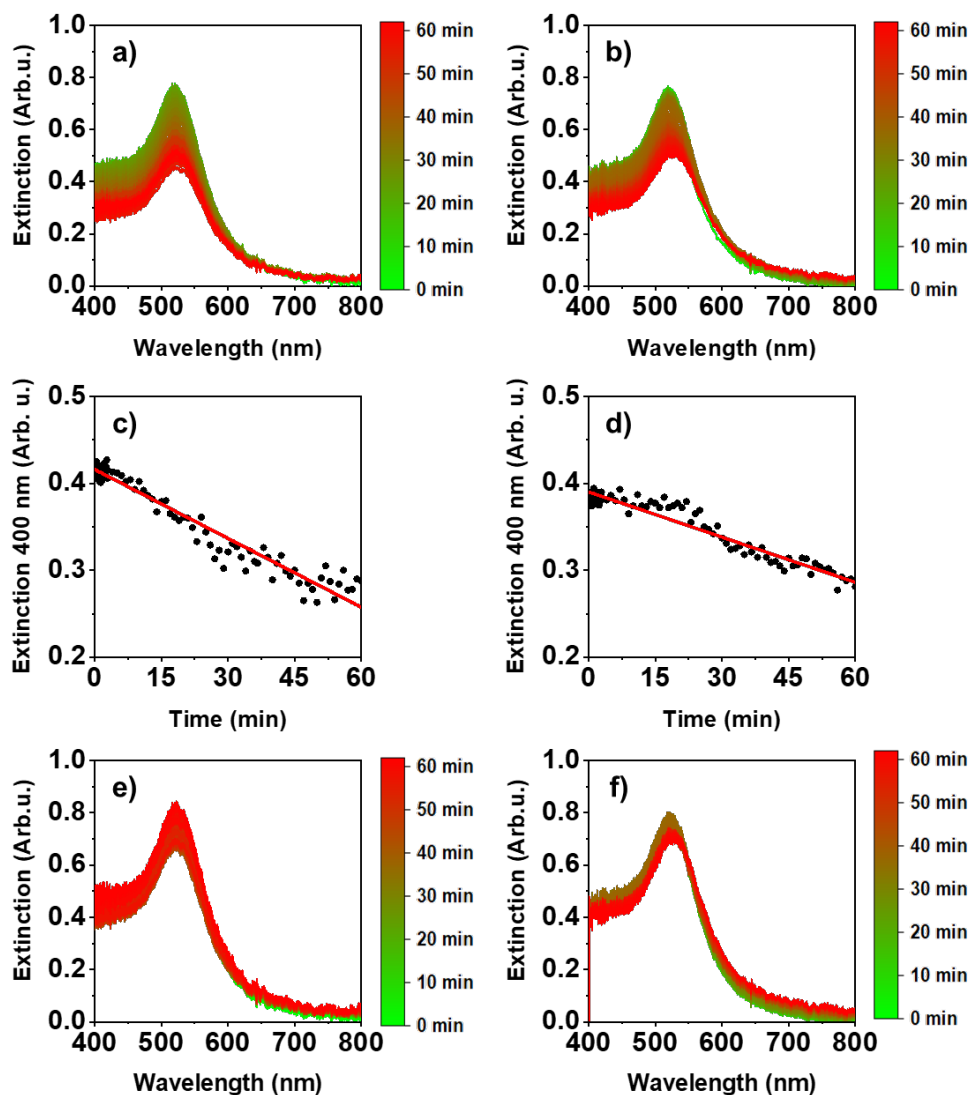


Figure S2: Time evolution of the ensemble extinction spectra when the ion concentration is 0.125 M, at 45 °C (a) and 55 °C (b). Decrease in extinction at 400 nm as a function of the elapsed time for 0.125 M, 45 °C (c) and 0.125 M, 55 °C (d). The linear fits are used for renormalization to obtain the corrected spectra e) 0.125 M, 45 °C and f) 0.125 M, 55 °C.

Simulation of the SAXS structure factor - $S(q)$

The simulated structure factor of the given arrangement of identical spherical scatterers was calculated according to the Debye scattering formula:

$$S(q) = 1 + \frac{2}{N} \sum_{i=1}^{N-1} \sum_{j=i+1}^N \frac{\sin(qr_{ij})}{qr_{ij}}$$

Based on the comparison of the calculated structure factor to the experimental one, the configuration of the particle clusters was systematically changed to obtain a best fit of the measurement result. Assuming isotropic interactions around the nanoparticles, a cluster containing 13 particles with compact arrangement was used; 12 particles surround a center particle. During the simulation the distance between the neighboring particles was adjusted. The particles can fluctuate around this equilibrium position along the x, y and z direction based on Gaussian distribution, resulting in different gaps (surface-to-surface distance) between the gold nanospheres; the standard deviation of this distribution is set as input parameter. The clustering rate is also accounted for by linearly combining the structure factor of the given clusters (renormalized with the number of particles in the cluster) with the structure factor of free particles $S(q)=1$. The weighting factor for the linear combination are α and $(1-\alpha)$ for the clustered and the free particles, respectively, that is α represents; the ratio of clustered to all particles in the system (e.g. at $\alpha=0.4$ 40% of the particles are incorporated in a cluster)

The number of particles in a cluster is an additional parameter used for tuning the structure factor to achieve the best fit. In a typical simulation 1000 measurements were performed and their average was compared to the experimental structure factor. **Figure S3** summarizes the effect of different input parameters on the calculated structure factor.

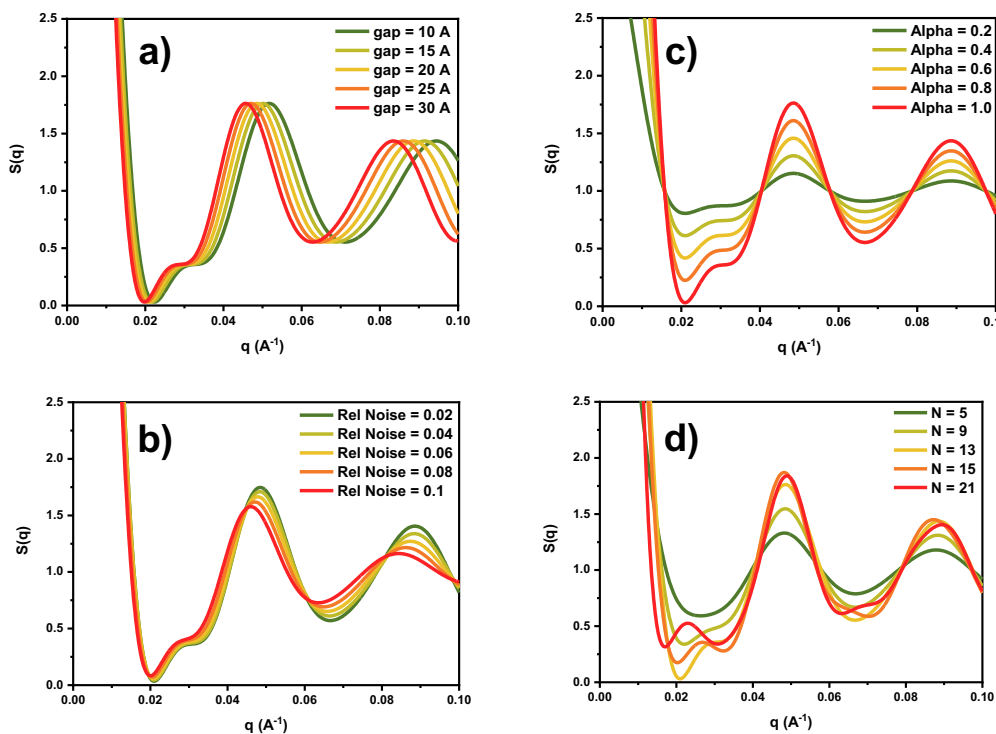


Figure S3: The effect of tuning a) interparticle distance, b) relative Gaussian noise, c) fraction of clustered particles and d) the number of particles on the calculated SAXS structure factor.

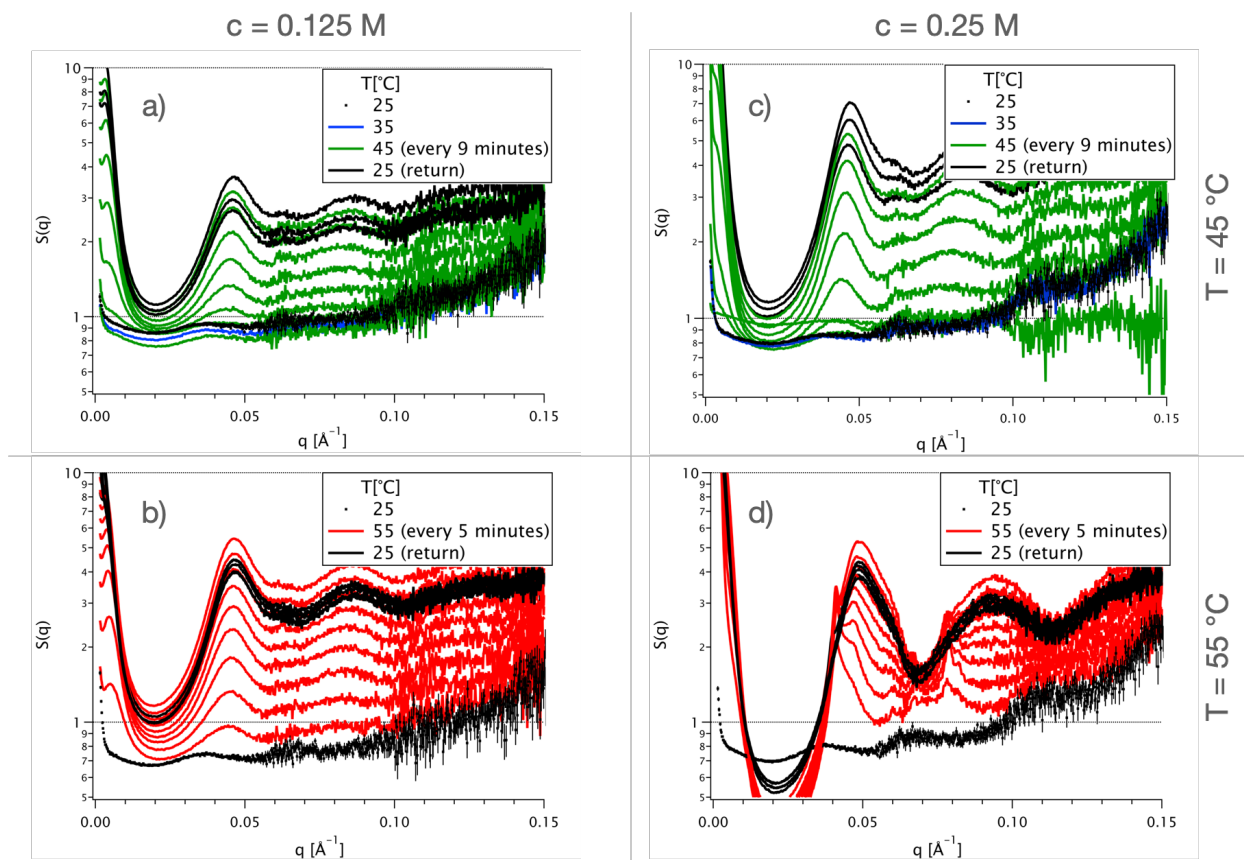


Figure S4: Time evolution of the structure factor obtained at different salt concentrations and temperatures. After clustering the system was returned to the initial temperature of 25 °C. The curves are shifted vertically for clarity.

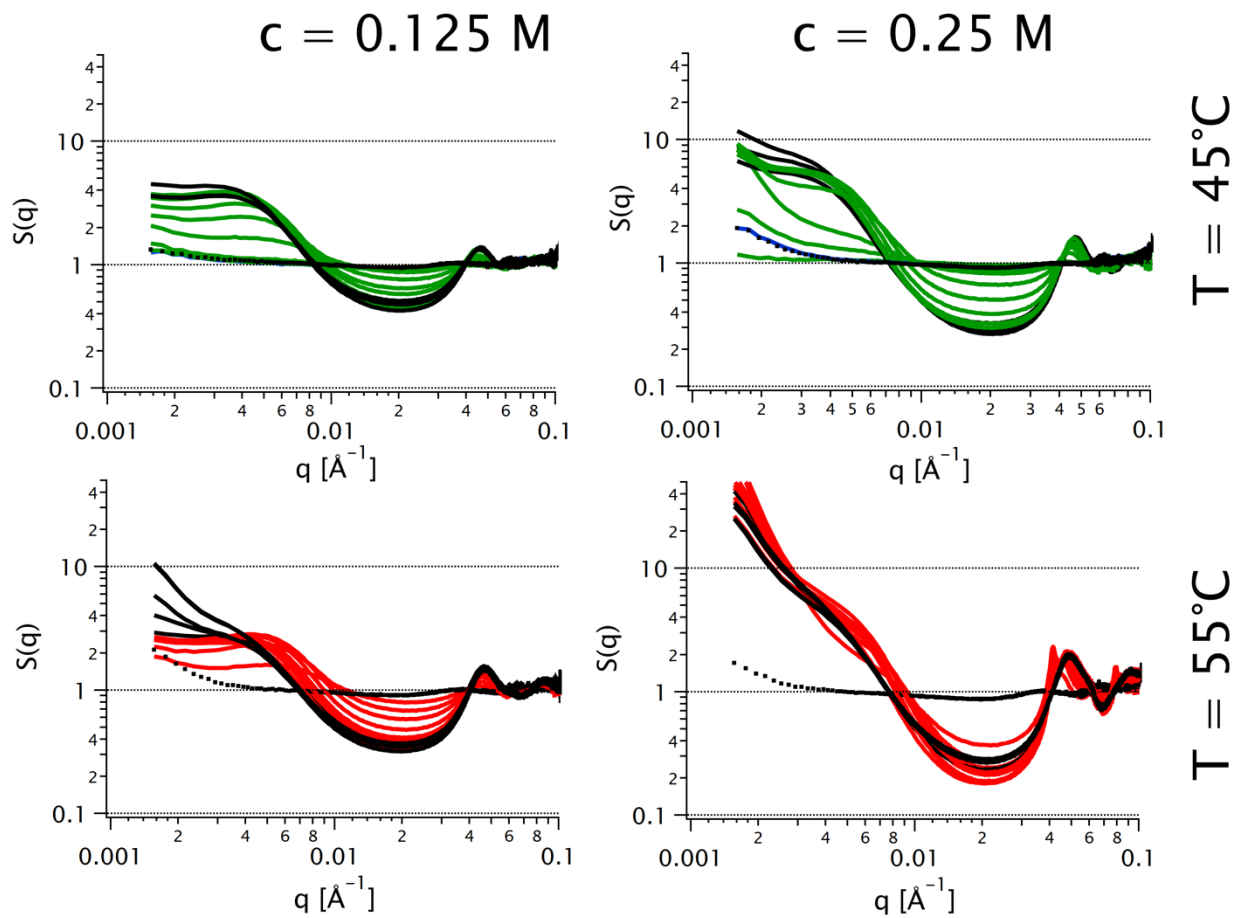


Figure S5: Same data as in Figure S4, but in log-log representation and without vertical shift.

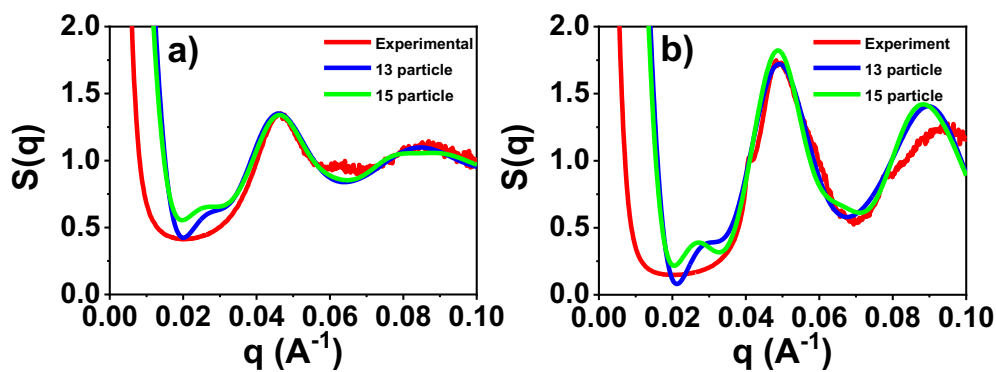


Figure S6: Experimental and calculated structure factors assuming 13 or 15 particles in the clusters for 0.125 M; 45 °C (a) and 0.25 M; 55 °C (b).

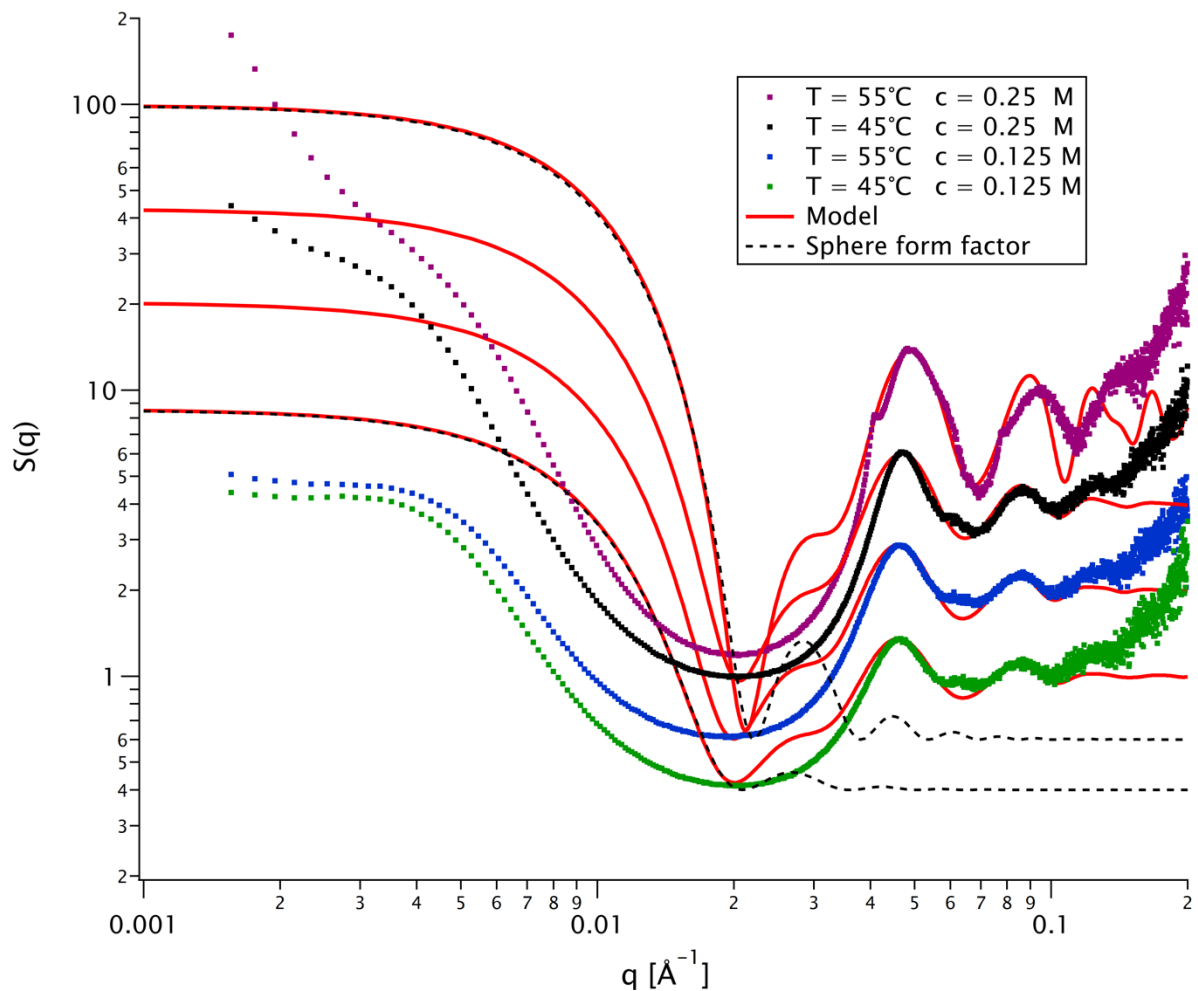
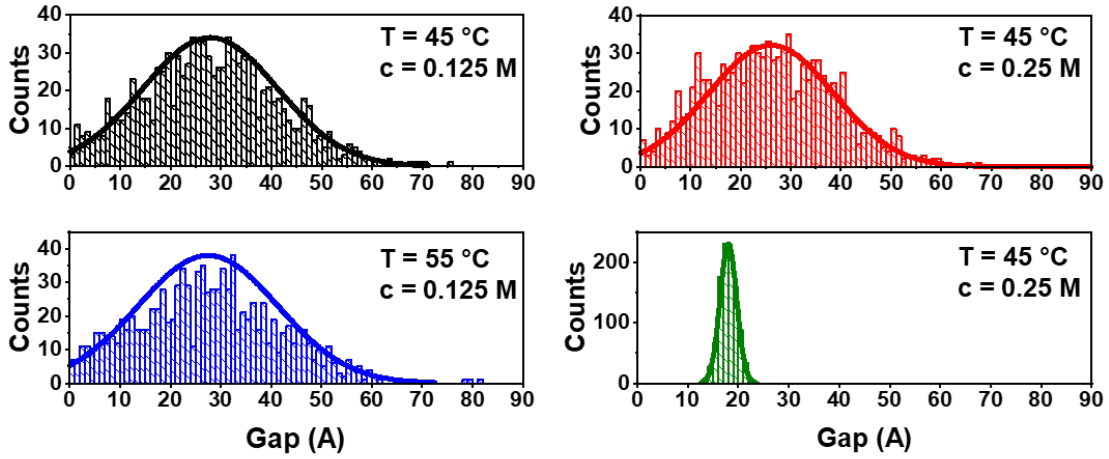


Figure S7: Experimental $S(q)$ (colored dots) and model (solid red lines) from Figure 3 in the main text, in log-log representation. The curves are shifted upwards by successive factors of 2. The form factor of a homogeneous sphere that best describes the small q range of the model is shown as dashed line for two curves.



Mean	Standard Deviation	Skewness	Kurtosis	Minimum	Median	Maximum
27.9	13.3	0.2	-0.2	0.4	27.4	75.3
26.0	12.4	0.2	-0.4	0.1	25.6	67.1
27.5	13.8	0.3	-0.1	0.1	27.4	81.3
18.0	1.7	0.0	-0.2	13.4	18.0	23.9

Figure S8: Distribution of interparticle distances at different temperatures and ion concentrations.

Colloidal interaction calculation

The colloidal pair interaction potential calculation was performed by summing up dispersion, electric double layer, and steric interaction terms:

$$U(D) = U_{disp}(D) + U_{EDL}(D) + U_{st}(D)$$

During calculations the SAXS derived particle size ($a=7.1$ nm) was used. Given the characteristic steep increase of the steric repulsion, for the effective PEG chain length the average surface separation distances obtained from SAXS (See Table 1 in the main text) have been divided by a factor of 2 and used as input in the calculation on the steric repulsion. For the as-prepared nanoparticles PEGylated particles zeta-potential of -9 mV was used. The dispersion interaction was calculated in the usual form of:

$$U_{Disp} = -\frac{A_{HAM}}{3} \left[\frac{a^2}{D(4a+D)} + \frac{a^2}{(2a+D)^2} + \frac{1}{2} \ln \left(1 - \frac{4a^2}{(2a+D)^2} \right) \right]$$

where a is the particle radius, D the surface-to-surface separation and A_{HAM} the Hamaker coefficient (2.5×10^{-19} J).¹ The electric double layer interaction was calculated based on effective scaled surface potentials,² steric interaction has been implemented as reported earlier.³ It has to be noted though, that at the investigated salt concentrations the repulsion contribution of electric double layer interaction to the total interaction is limited and the net pair-interaction is dominated by the interplay between the attractive dispersion and repulsive steric interaction. This is clear if one compares the Debye length (κ^{-1}) with the native PEG brush thickness. The former can be calculated based on the concentration of used 1:2 electrolyte (Figure S7, right) and shows that at 0.125 and 0.25 M concentration the Debye length is well below 1 nm.⁴ While the plotted values are calculated at 25°C, at the highest temperature investigated (55°C) these

increase only marginally (from 0.50 to 0.52 nm at 0.125M and from 0.35 to 0.37 nm at 0.25 M, respectively). In comparison, the native PEG brush thickness on the as-prepared nanoparticles extends much further; around 1.85 ± 0.1 nm, as derived earlier from dynamic light scattering experiments for the same system.³ The brush type PEG-graft on the Au spheres due the high grafting density (above $4/\text{nm}^2$) was shown in an earlier literature report based on DLS and TGA measurements.⁵

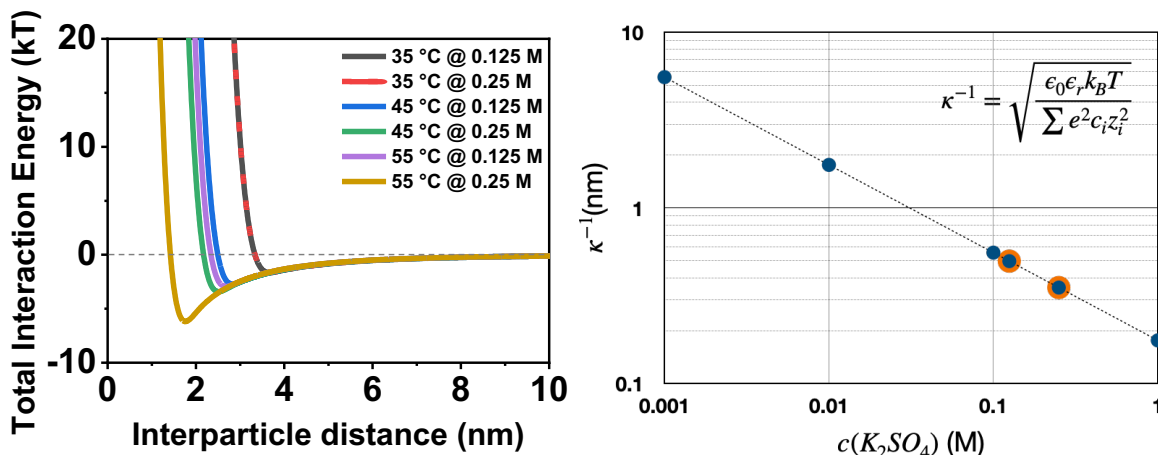


Figure S9: Calculated total interaction energy at different temperatures and salt concentrations (left). Log-log plot of the calculated Debye length (κ^{-1}) at 25 °C as a function of the 1:2 electrolyte concentration (right). The two orange-colored points mark the concentration values used during the experiments (0.125 and 0.25M, respectively).

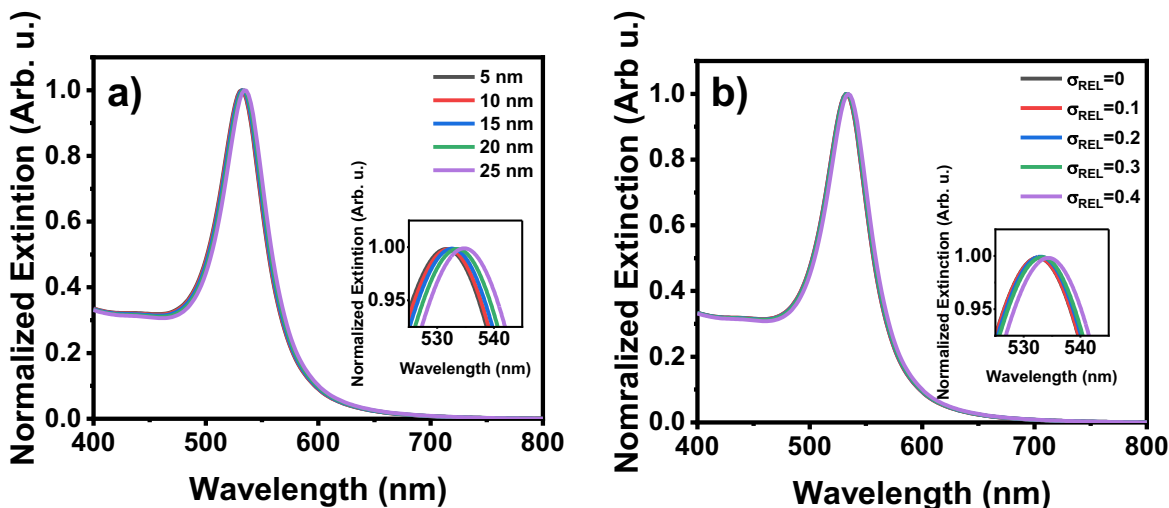


Figure S10: Calculated extinction spectra of spherical gold nanoparticles with different size from 5 nm to 25 nm (a). Simulated mean extinction spectra of particles with different standard deviation (b). The insets show the zoomed graph of the extinction spectra close to the resonance peak.

References

- 1 S. Biggs and P. Mulvaney, *The Journal of Chemical Physics*, 1994, **100**, 8501–8505.
- 2 Y. Zheng, L. Rosa, T. Thai, S. H. Ng, D. E. Gómez, H. Ohshima and U. Bach, *Journal of Materials Chemistry A*, 2015, **3**, 240–249.
- 3 D. Zámbo, G. Z. Radnóczy and A. Deák, *Langmuir*, 2015, **31**, 2662–2668.
- 4 J. N. Israelachvili, *Intermolecular and surface forces*, Academic Press, Burlington, MA, 3rd ed., 2011.
- 5 K. Rahme, L. Chen, R. G. Hobbs, M. A. Morris, C. O’Driscoll and J. D. Holmes, *RSC Advances*, 2013, **3**, 6085.